

# Real-Time Dedispersion for Fast Radio Transient Surveys, using Auto Tuning on Many-Core Accelerators

Alessio Sclocco<sup>a,b</sup>, Joeri van Leeuwen<sup>b,c</sup>, Henri E. Bal<sup>a</sup>, Rob V. van Nieuwpoort<sup>d</sup>

<sup>a</sup>Faculty of Sciences, Vrije Universiteit Amsterdam, Amsterdam, the Netherlands

<sup>b</sup>ASTRON, the Netherlands Institute for Radio Astronomy, Dwingeloo, the Netherlands

<sup>c</sup>Astronomical Institute “Anton Pannekoek”, University of Amsterdam, Amsterdam, the Netherlands

<sup>d</sup>NLeSC, Netherlands eScience Center, Amsterdam, the Netherlands

---

## Abstract

Dedispersion, the removal of deleterious smearing of impulsive signals by the interstellar matter, is one of the most intensive processing steps in any radio survey for pulsars and fast transients. We here present a study of the parallelization of this algorithm on many-core accelerators, including GPUs from AMD and NVIDIA, and the Intel Xeon Phi. We find that dedispersion is inherently memory-bound. Even in a perfect scenario, hardware limitations keep the arithmetic intensity low, thus limiting performance. We next exploit auto-tuning to adapt dedispersion to different accelerators, observations, and even telescopes. We demonstrate that the optimal settings differ between observational setups, and that auto-tuning significantly improves performance. This impacts time-domain surveys from Apertif to SKA.

*Keywords:* Pulsars: general – Astronomical instrumentation, methods and techniques – Techniques: miscellaneous

---

## 1. Introduction

Astronomical phenomena such as pulsars (Hewish et al., 1968) and fast radio bursts (FRBs; Lorimer et al., 2007) consist of millisecond-duration impulsive signals over a broad radio-frequency range. As the electromagnetic waves propagate through the interstellar material (ISM) between us and the source, they are dispersed (Lorimer and Kramer, 2005). This causes lower radio frequencies to arrive progressively later, and without correction this results in a loss of signal-to-noise, that often makes the source undetectable when integrating over a wide observing bandwidth. This frequency-dependent delay can be removed in a process called *dedispersion*. Complete removal can be achieved by reverting all phases through a convolution of the signal with the inverse of the modeled ISM (coherent dedispersion; Hankins and Rickett, 1975). Incomplete but much faster removal, especially when many dispersion measure trials are required, can be achieved by appropriately shifting in time the signal frequency channels (incoherent dedispersion; from now on referred to plainly as dedispersion). This dedispersion is a basic algorithm in high-time-resolution radio astronomy, and one of the building blocks of surveys for fast phenomena with modern radio telescopes such as the Low Frequency Array (LOFAR; van Leeuwen and Stappers, 2010; Stappers et al., 2011) and the Square Kilometer Array (SKA; Carilli

and Rawlings, 2004). In these surveys, the dispersion measures are a priori unknown, and can only be determined in a brute-force search. This search generally runs on off-site supercomputers. These range from e.g., the CM-200 in the Foster et al. (1995) Arecibo survey, to gSTAR for the Parkes HTRU (Keith et al., 2010), and Cartesius for the LOFAR LOTAAS (Coenen et al., 2014) surveys. In the latter the dedispersion step amounts to over half of all required pulsar-search processing. For the SKA, this processing will amount to many PFLOPS for both SKA-Mid (cf. Magro, 2014) and SKA-Low (Keane et al., 2014).

Above and beyond these pure compute requirements, the similar and often simultaneous search for FRBs demands that this dedispersion is done near real time. Only then can these fleeting events be immediately followed up by telescopes at other energies (Petroff et al., 2015).

We aim to achieve the required performance by parallelizing this algorithm for many-core accelerators. Compared to similar attempts made by Barsdell et al. (2012) and Armour et al. (2012), we present a performance analysis that is more complete, and introduce a novel many-core algorithm that can be tuned for different platforms and observational setups. To our knowledge, this is the first attempt at designing a brute-force dedispersion algorithm that is highly portable and not fine-tuned for a specific platform or telescope.

To summarize our contributions, in this paper we: (1) provide an in-depth analysis of the arithmetic intensity (AI) of brute-force dedispersion, finding analytically and empirically that it is memory bound; (2) show that auto-tuning can adapt the algorithm to different platforms, tele-

---

*Email addresses:* a.sclocco@vu.nl (Alessio Sclocco), leeuwen@astron.nl (Joen van Leeuwen), h.e.bal@vu.nl (Henri E. Bal), r.vannieuwpoort@esciencecenter.nl (Rob V. van Nieuwpoort)

scopes, and observational setups; (3) demonstrate that many-core accelerators can achieve real-time performance; (4) quantify the impact that auto-tuning has on performance; (5) compare different platforms using a real-world scientific application; and (6) compare the performance of OpenCL and OpenMP for the Intel Xeon devices.

In Section 2 we describe the brute-force dedispersion algorithm, our parallel implementation and its optimizations; and the theoretical analysis of the dedispersion AI. We next present our experiments (Section 3), results (Section 4) and further discussion (Section 5). Finally, relevant literature is discussed in Section 6, and Section 7 summarizes our conclusions.

## 2. The Brute-Force Dedispersion Algorithm

In dispersion (Lorimer and Kramer, 2005), the highest frequency in a certain band  $f_h$  is received at time  $t_x$ , while lower simultaneously emitted frequency components  $f_i$  arrive at  $t_x + k$ . For frequencies expressed in MHz this delay in seconds is:

$$k \approx 4150 \times DM \times \left( \frac{1}{f_i^2} - \frac{1}{f_h^2} \right) \quad (1)$$

Here the Dispersion Measure  $DM$  represents the projected number of free electrons between the source and the receiver. In incoherent dedispersion, the lower frequencies are shifted in time and realigned with the higher ones, thus approximating the original signal.

In a survey, the incoming signal must be brute-force dedispersed for thousands of possible DM values. As every telescope pointing direction or *beam* can be processed independently, performance of the dedispersion algorithm can be improved by means of large-scale parallelization.

### 2.1. Sequential Algorithm

The input of this algorithm is a frequency-channelized time series, represented as a  $c \times t$  matrix, with  $c$  frequency channels and  $t$  time samples needed to dedisperse one second of data. The output is a set of  $d$  dedispersed trial-DM time-series, each of length  $s$  samples per second, represented as a  $d \times s$  matrix. All data are single precision floating point numbers; their real-life rates are e.g. 36 GB/s input and 72 GB/s output for the pulsar search with AperiTif on the Westerbork telescope (van Leeuwen, 2014).

Dedispersion (sequential pseudocode shown in Algorithm 1) then consists of three nested loops, and every output element is the sum of  $c$  samples: one for each frequency channel. Which samples are part of each sum depends on the applied delay (i.e.  $\Delta$ ) that, as we know from Equation 1, is a non-linear function of frequency and DM. These delays can be computed in advance, so they do not contribute to the algorithm's complexity. Therefore, the complexity of this algorithm is  $O(d \times s \times c)$ .

In the context of many-core accelerators, there is another, extremely important algorithmic characteristic: the

---

**Algorithm 1** Pseudocode of the brute-force dedispersion algorithm.

---

```

for dm = 0  $\rightarrow$  d do
  for sample = 0  $\rightarrow$  s do
    dSample = 0
    for chan = 0  $\rightarrow$  c do
      dSample += input[chan][sample +  $\Delta$ (chan, dm)]
    end for
    output[dm][sample] = dSample
  end for
end for

```

---

*Arithmetic Intensity* (AI), i.e. the ratio between the performed floating-point operations and the number of bytes accessed in global memory. In many-core architectures the gap between computational capabilities and memory bandwidth is wide, and a high AI is thus a prerequisite for high performance (Williams et al., 2009). Unfortunately, the AI for Algorithm 1 is inherently low, with only one floating point operation per four bytes loaded from global memory. For dedispersion,

$$AI = \frac{1}{4 + \epsilon} < \frac{1}{4} \quad (2)$$

where  $\epsilon$  represents the effect of accessing the delay table and writing the output. This low AI shows that brute-force dedispersion is memory bound on most architectures. Its performance is thus limited not by computational capabilities, but by memory bandwidth. One way to increase AI and thus improve performance, is to reduce the number of reads from global memory, by implementing some form of data reuse. In Algorithm 1 some data reuse appears possible. For some frequencies, the delay is the same for two close DMs,  $dm_i$  and  $dm_j$ , so that  $\Delta(c, dm_i) = \Delta(c, dm_j)$ . Then, one input element provides two different sums. With data reuse,

$$AI < \frac{d \times s \times c}{4 \times ((s \times c) + (d \times s) + (d \times c))} = \frac{1}{4 \times (\frac{1}{d} + \frac{1}{s} + \frac{1}{c})} \quad (3)$$

The bound from Equation 3 theoretically goes toward infinity, but in practice the non-linear delay function diverges rapidly at lower frequencies. There is never enough data reuse to approach the upper bound of Equation 3; for a more in-depth discussion see Sclocco et al. (2014). We thus categorize the algorithm as memory-bound. In this conclusion we differ from previous literature such as Barsdell et al. (2010) and Barsdell et al. (2012). The importance of the above mentioned data reuse in dedispersion was identified early on and implemented in e.g. the tree dedispersion algorithm (Taylor, 1974). That fast implementation has the drawback of assuming the dispersion sweep is linear. Several modern pulsar and FRB surveys with large fractional bandwidths have used modified tree algorithms that sum over the *quadratic* nature of the sweep (e.g. Manchester et al. (2001), Masui et al. (2015)).

### 2.2. Parallelization

We first determine how to divide and organise the work of different threads, and describe these in OpenCL ter-

minology. We identify three main algorithm dimensions: DM, time and frequency. Time and DM are independent, and ideal for parallelization, avoiding any inter- and intra-thread dependency. In our implementation, each OpenCL work-item (i.e. thread) is associated with a different (DM, time) pair and it executes the innermost loop of Algorithm 1. An OpenCL work-group (i.e. group of threads) combines work-items that are associated with the same DM, but with different time samples.

This proposed organization also simplifies memory access, using coalesced reads and writes. Different small requests can then be combined in one bigger operation. This well-known optimization is a performance requisite for many-core architectures, especially for memory-bound algorithms like dedispersion. Our output elements are written to adjacent, and aligned, memory locations. The *reads* from global memory are also coalesced but, due to the shape of the delay function, are not always aligned. The worst-case memory overhead is at most a factor two (Sclocco et al., 2014).

To exploit data reuse, we compute more than one DM per work-group. So, the final structure of our many-core dedispersion algorithm consists of two-dimensional work-groups. In this way a work-group is associated with more than one DM, so that its work-items can either collaborate to load the necessary elements from global to *local memory* (a fast memory area that is shared between the work-items of a same work-group) or rely on the cache.

The general structure of the algorithm can be specifically instantiated by configuring five user-controlled parameters. Two parameters control the number of work-items per work-group in the time and DM dimensions, thus regulating parallelism. Two parameters control the number of elements per work-item. The last parameter specifies whether local memory or cache are employed for data reuse. These parameters determine source code generation at run time. Because we do not know, a priori, the optimal configuration of these parameters, we rely on auto-tuning, i.e. we try all meaningful combinations and select the best performing one.

### 3. Experimental Setup

In this section we describe how the experiments are carried out; all information necessary for replication is detailed in Sclocco et al. (2014). Table 1 lists the platforms used, and reports basic details such as number of OpenCL Compute Elements (CEs) (i.e. cores), peak performance, peak memory bandwidth and thermal design power (TDP).

We run the same code on every many-core accelerator; the source code<sup>1</sup> is implemented in C++ and OpenCL. The accelerators are part of the Distributed ASCI Supercomputer 4 (DAS-4)<sup>2</sup>. As dedispersion is usually part of

Platform	CEs	GFLOP /s	GB /s	Watt
AMD HD7970	64 × 32	3,788	264	250
NVIDIA GTX 680	192 × 8	3,090	192	195
NVIDIA GTX Titan	192 × 14	4,500	288	250
NVIDIA K20	192 × 13	3,519	208	225
Intel Xeon Phi 5110P	2 × 60	2,022	320	225
Intel Xeon E5-2620	6 × 1	192	42	95

Table 1: Characteristics of the used platforms.

Survey	s (Hz)	BW (MHz)	n <sub>chan</sub>	f (MHz)
LOFAR	200,000	6	32	138–145
Apertif	20,000	300	1,024	1,420–1,729

Table 2: Survey name, sampling rate  $s$ , bandwidth  $BW$ , total number of channels  $n_{chan}$  and frequency range  $f$  for the two experimental setups.

a larger pipeline, input and output are assumed to reside on the device. We thus do not measure data transfers over the PCI-e bus.

The experimental set ups (Table 2) are based on two different pulsar surveys, one for a hypothetical high-time resolution LOFAR survey comparable to the LOFAR Pilot Pulsar Survey (Coenen et al., 2014) and one for the planned Apertif pulsar/FRB survey (van Leeuwen, 2014). For both, trial DMs start at 0 and increment by 0.25  $pc/cm^3$ . These two setups stress different characteristics of the algorithm – the Apertif setup, at 20 MFLOP per DM, is three times more compute intensive than LOFAR at 6 MFLOP per DM. Yet the higher Apertif frequencies cause reduced delays, with more potential for data reuse. We thus try two complementary scenarios: one is more computationally intensive, but potentially offers more data reuse, and one that is less computationally intensive, but precludes almost any data reuse.

We auto-tune the five algorithm parameters described in Section 2, for each of the six platforms of Table 1, in both observational setups. We use 12 different input instances between 2–4,096 (Sclocco et al., 2014), and measure our performance metric, the number of single precision floating-point operations per second.

### 4. Results

#### 4.1. Auto-Tuning

For the Apertif case, the optimal number of work-items per work-group identified by auto-tuning is the highest for the GTX 680 (1,024). The other three GPUs require between 256 and 512, while the two Intel platforms require the lowest number (i.e. between 16 and 128). As detailed in Sclocco et al. (2014), the optimal configuration is more variable with smaller input instances, where optimization space is small.

Results for the LOFAR setup are more stable. It has less available data reuse, easing the identification of the optimum. The number of work-items per work-group stay

<sup>1</sup><https://github.com/isazi/Dedispersion>

<sup>2</sup><http://www.cs.vu.nl/das4/>

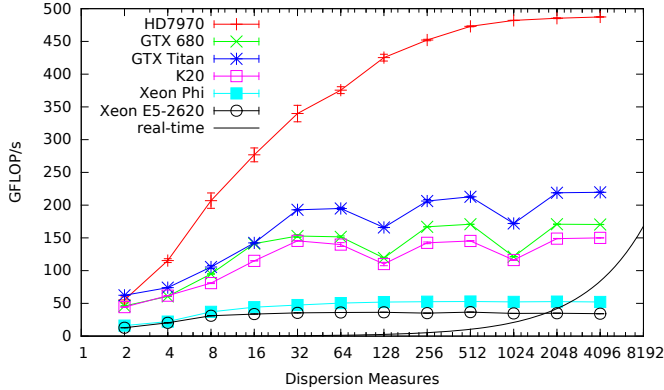


Figure 1: Performance of auto-tuned dedispersion, Apertif (higher is better).

similar for the GPUs, and is somewhat lowered for the Intel platforms.

Even for similar total numbers of work-items per work-group, the two underlying parameters (Section 2) may differ. For e.g. the HD7970, the Apertif work-group is as  $8 \times 32$  work-items, while LOFAR it is composed by  $64 \times 4$  work-items. In the Apertif setup the auto-tuning identifies a configuration that intensively exploits the available data reuse, while in the LOFAR setup the optimal configuration relies more on the device occupancy.

This result is important: accelerated dedispersion algorithm has no single optimal configuration – it must be adapted to the exact observational setup.

The subsequent auto tuning the amount of work per work-item again exploits each accelerator’s advantage, such as the high number of registers in the K20 and Titan, adapting the algorithm to different scenarios (Sclocco et al., 2014).

The last tunable parameter is the explicit use of local memory, present on the GPUs, to exploit data reuse, over just hardware cache. Again auto-tuning adjusted the interaction of different parameters for highest performance dedispersion in each platform.

In summary, we find that optimal configurations cannot be identified a priori, and that auto-tuning is the only feasible way to properly configure the dedispersion algorithm, because of the number and interaction of parameters, and their impact on AI.

#### 4.2. Impact of Auto-Tuning on Performance

In Fig. 1 we show the performance achieved by auto-tuned dedispersion for the Apertif case. All platforms show a performance increase with the dimension of the input instance, and plateauing afterwards. Note how the tuned algorithm scales better than linearly up to this maximum, and then scales linearly. The HD7970 achieves highest performance, the Intel CPU and the Xeon Phi are at the bottom, and the three NVIDIA GPUs occupy the middle of this figure. On average, the HD7970 is 2.7 times faster than the NVIDIA GPUs, and 11.3 times faster than

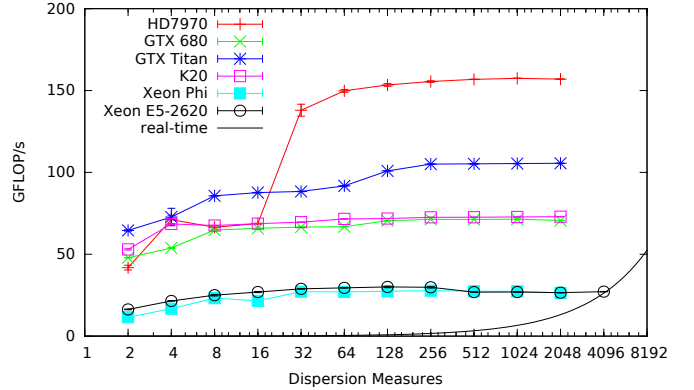


Figure 2: Performance of auto-tuned dedispersion, LOFAR (higher is better).

the Intel CPU and Xeon Phi; the Phi is 1.5 times faster than the multi-core CPU.

The results for the LOFAR scenario (Fig. 2) are different. Absolute performance is lower. This is caused by the reduced available data reuse, resulting in lower algorithm AI. Next, the GPUs are closer in performance; now the HD7970 is only 1.4 times faster than the GTX Titan. With less data reuse available, memory bandwidth becomes increasingly more important, leveling the differences. On average, the HD7970 is just 1.9 times faster than the NVIDIA GPUs, and 6 times faster than the Intel CPU and Xeon Phi.

In both figures, only scenarios above the “real-time” line can dedisperse one second of data in less than one second of computation. This is a fundamental requirement for modern radio telescopes, whose extreme data rate precludes data storage and off-line processing. We show that GPUs can scale to bigger instances and/or to a multi-beam scenario, and still satisfy the real-time constraints.

What was the impact of auto-tuning on performance? Figure 3 shows the histogram of performance in the optimization space. The optimum lies far from the typical configuration. Because optimal configurations depends on multiple parameters, like the platform used to execute the algorithm, and specific observational parameters, it will not be trivial, even for an experienced user, to manually select the best configuration without extensive tuning. This claim is also supported by the high signal-to-noise ratio of the optimal configurations, as detailed in Sclocco et al. (2014).

In summary, we satisfy a realistic real-time constraint in almost every test case, which allows for massive multi-beaming. Optimal configurations are difficult to guess in this optimization space, and therefore auto-tuning has a critical impact on the performance.

#### 4.3. Data Reuse and Performance Limits

To simulate a scenario with perfect data reuse, we tune and measure the performance of dedispersion using the value zero for all DM trials. In the case of For Apertif, the

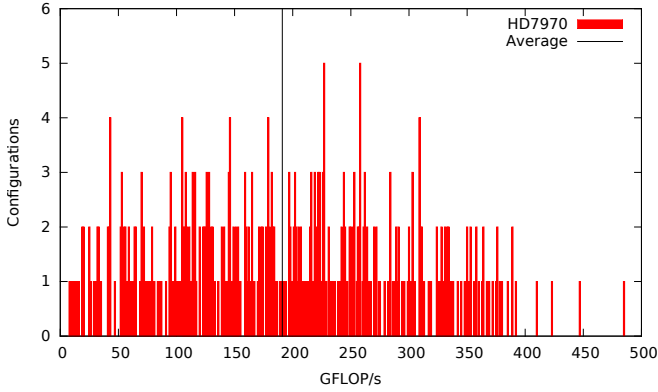


Figure 3: Example of a performance histogram, for the case of Apertif 2,048 DMs.

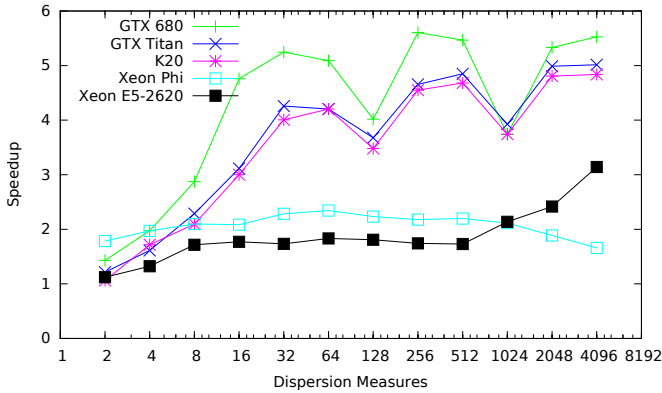


Figure 4: Speedup over a generically tuned configuration, Apertif (higher is better). The HD7970 GPU is missing because there are no valid configurations of the algorithm that do not exploit data reuse.

difference is negligible (cf. Fig. 11 in Sclocco et al. 2014). Data reuse was already maximized. For the LOFAR setup (cf. Fig. 12 in Sclocco et al. 2014), the performance improves, approaching the Apertif setup. The increased data reuse is exploited until the hardware is saturated.

Performance is predominantly determined by the amount of possible data reuse, which is a function of real-life frequencies and DM values. This tests our hypothesis that even with perfect data reuse, high AI cannot be achieved because of the limitations of real hardware (in contrast with the conclusions of Barsdell et al. 2010). We therefore conclude that brute-force dedispersion is memory-bound for every practical and realistic scenario.

## 5. Discussion

We first compare the performance of the *auto-tuned* versus a *generically tuned* algorithm. In the latter, tuning is confined to a mono-dimensional configuration of the workgroups and the work-items compute only one DM value. This strategy is widely applied by programmers; but as the algorithm’s AI is unaffected, data reuse is not optimized.

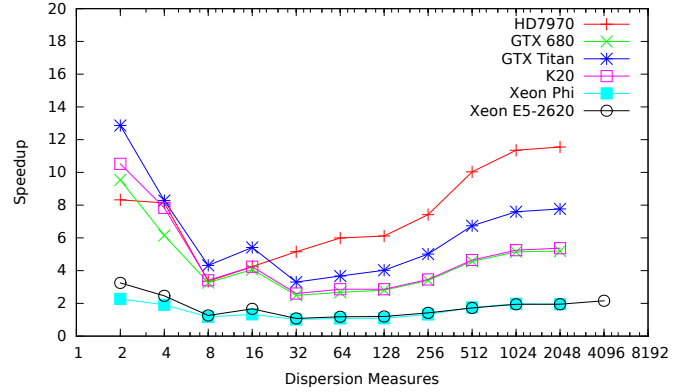


Figure 5: Speedup over a parallel CPU implementation, LOFAR (higher is better).

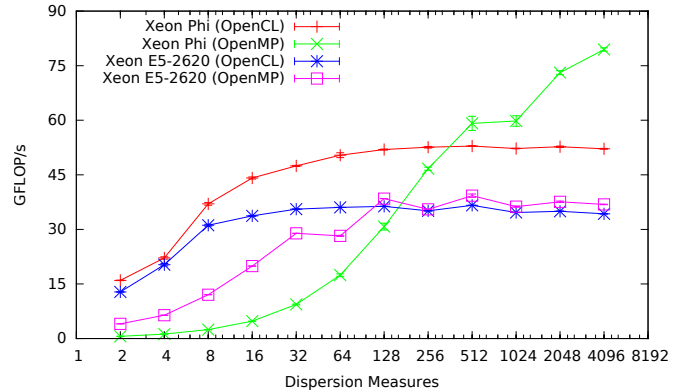


Figure 6: Comparing OpenCL and OpenMP implementations on the CPU and Xeon Phi, Apertif (higher is better).

We find that *auto-tuned* dedispersion on GPUs is  $\sim 5$  times faster than *generically tuned* in the Apertif setup (Fig. 4), and still 1.5–2.5 times faster in the LOFAR setup. Effectively exploiting data reuse is a main performance driver for a high-performance dedispersion algorithm, especially for those platforms where the gap between floating point peak performance and memory bandwidth is wide.

We also compare the performance of our auto-tuned algorithm to an optimized CPU version. This CPU version of the algorithm is parallelized using OpenMP instead of OpenCL, with different threads computing different chunks of DM values and time samples. It includes all meaningful optimizations described in Section 2.2, and is vectorized using Intel’s Advanced Vector Extensions (AVX) intrinsics. Like the OpenCL version, it is automatically auto-tuned. For both observational setups (cf. Fig. 5 for LOFAR), the many-core implementation is considerably faster than a highly optimized, and tuned, CPU implementation.

The OpenMP code generator was also extended to generate native code for the Xeon Phi, and we compared the Intel CPU and Xeon Phi, using both OpenCL and OpenMP. In the Apertif case (Figure 6) the OpenCL im-

plementation is faster than the OpenMP one for smaller inputs, while the opposite is true for larger ones, and this behavior holds for both platforms. In the LOFAR case, however, this same behavior applies only to the Xeon Phi, with the Xeon E5-2620 showing a performance degradation for bigger inputs that is consistent with the experiments of Armour et al. (2012). Overall improvements to the Intel OpenCL compiler could improve the Xeon Phi’s performance, as we were able to achieve a 51% improvement in performance on this platform using a tuned OpenMP implementation.

### 5.1. Multi-Beam Performance

In the conclusions of Section 4.2 we highlighted how dedispersion performance can allow for multi-beam scenarios. Apertif will need to dedisperse 2,000 DMs in real-time for 450 different beams, thus requiring 18.5 TFLOP/s just for dedispersion. Using our best performing accelerator, the AMD HD7970, it is possible to dedisperse 2,000 DMs in 0.08 seconds; 9 beams per GPU could be dedispersed in real-time. Enough memory is available. Therefore, the 18.5 TFLOP/s dedispersion instrument for Apertif could be implemented using 2015 technology with  $\sim$ 50 GPUs. With a HD7970 model with double the memory, 12 beams could be dedispersed at once, reducing the system size to only 38 GPUs.

For its real-life impact, we compute an upper bound on the power necessary for dedispersion on Apertif from the TDPs (Table 1): the proposed GPU solution requires 12.5 kW while the traditional CPU solution requires 46.5 kW. We can therefore conclude that, in this scenario, using many-core accelerators does not only provide a 9.8 times reduction in the size of the system, when compared to a traditional CPU-based solution, but it also lowers the power consumption by a factor of 3.7. This improvement in energy efficiency is in part architectural, and in part caused by auto-tuning. Using the results of Section 4.2 it is possible to determine that the power that would be required by an average configuration is 22.5 kW: we can thus conclude that auto-tuning is responsible for around 50% of the total power savings.

## 6. Related Work

In the literature, auto-tuning is considered a viable technique to achieve performance that is both high and portable. In particular, Li et al. (2009) show that it is possible to use auto-tuning to improve performance of even highly-tuned algorithms, and Datta et al. (2008) affirm that application specific auto-tuning is the most practical way to achieve high performance on multi-core systems. Highly relevant here is the work of Du et al. (2012), with whom we agree that auto-tuning can be used as a performance portability tool, especially with OpenCL. Another attempt at achieving performance portability on heterogeneous systems has been made by Phothilimthana et al.

(2013), and while their approach focuses on the compiler, it still relies on auto-tuning to map algorithms and heterogeneous platforms in an optimal way. In recent years, we have been working on parallelizing and implementing radio astronomy kernels on multi and many-core platforms (van Nieuwpoort and Romein, 2011), and using auto-tuning to achieve high performance on applications like the LOFAR beam former (Sclocco et al., 2012). What makes our current work different, is that we do not only use auto-tuning to achieve high performance, but measure its impact, and show that the optimal configurations are difficult to guess without thorough tuning.

While there are no previous attempts at auto-tuning dedispersion for many cores, there are a few previous GPU implementations documented in literature. First, in Barsdell et al. (2010) dedispersion is listed as a possible candidate for acceleration, together with other astronomy algorithms. While we agree that dedispersion is a potentially good candidate for many-core acceleration because of its inherently parallel structure, we believe their performance analysis to be too optimistic, and the AI estimate in Barsdell et al. (2010) to be unrealistically high. In fact, we showed in this paper that dedispersion’s AI is low in all realistic scenarios, and that the algorithm is inherently memory-bound. The same authors implemented, in a follow-up paper (Barsdell et al., 2012), dedispersion for NVIDIA GPUs, using CUDA as their implementation framework. However, we do not completely agree with the performance results presented in Barsdell et al. (2012) for two reasons: first, they do not completely exploit data reuse, and we have shown here how important data reuse is for performance; and second, part of their results are not experimental, but derived from performance models.

Another GPU implementation of the dedispersion algorithm is presented in Magro et al. (2011). Also in this case there is no mention of exploiting data reuse. In fact, some of the authors of this paper published, shortly after Magro et al. (2011), another short paper (Armour et al., 2012) in which they affirm that their previously developed algorithm does not perform well enough because it does not exploit data reuse. Unfortunately, this paper does not provide sufficient detail on either the algorithm or on experimental details, such as frequencies and time resolution, for us to repeat their experiment. Therefore, we cannot verify the claimed 50% of theoretical peak performance. However, we believe this claim to be unrealistic because dedispersion has an inherently low AI, and it cannot take advantage of fused multiply-adds, which by itself already limits the theoretical upper bound to 50% of the peak on the used GPUs.

A different approach to both brute-force and tree based dedispersion has been proposed by Zackay and Ofek (2014). This new algorithm has lower computational complexity than brute-force dedispersion, and appears to be faster than the implementations of both Magro et al. (2011) and Barsdell et al. (2012). Although the experimental results highlighted in our paper show higher per-

formance than the results presented in Zackay and Ofek (2014), we believe this algorithm has potential; and that it, too, could benefit from auto-tuning to further improve performance in real-life implementations.

## 7. Conclusions

In this paper, we analyzed the brute-force dedispersion algorithm, and presented our many-core implementation. We analytically proved that dedispersion is a memory-bound algorithm and that, in any real world scenario, its performance is limited by low arithmetic intensity. With the experiments presented in this paper, we also demonstrated that by using auto-tuning it is possible to obtain high performance for dedispersion. Even more important, we showed that auto-tuning makes the algorithm portable between different platforms and different observational setups. Furthermore, we highlighted how auto-tuning permits to automatically exploit the architectural specificities of different platforms.

Measuring the performance of the tuned algorithm, we verified that it scales linearly with the number of DMs for every tested platform and observational setup. So far, the most suitable platform to run dedispersion among the ones we tested, is a GPU from AMD, the HD7970. This GPU performs 2–9 times better than the other accelerators when extensive data reuse is available, and remains 1.4–6 times faster even in less optimal scenarios. Overall, the GPUs are 4.9–7.5 and 3.8 times faster than the CPU and Xeon Phi in the two scenarios analyzed in this work. We conclude that, at the moment, GPUs are the best candidate for brute-force dedispersion.

In this paper, we showed that using the HD7970 GPU it would be possible to build the 18.5 TFLOP/s dedispersion instrument for Apertif using just  $\sim 50$  accelerators, thus reducing the system size of a factor 9.8 and the power requirements of a factor 3.7. These improvements are only in part architectural, and mostly a result of optimal tuning of the algorithm. We will continue to compare platforms as the design date for SKA approaches.

Another important contribution of this paper is the quantitative evidence of the impact that auto-tuning has on performance. With our experiments, we showed that the optimal configuration is difficult to find manually and lies far from the average. Moreover, we showed that the auto-tuned algorithm is faster than a generically tuned version of the same algorithm on all platforms, and is an order of magnitude faster than an optimized CPU implementation.

Finally, our last contribution was to provide further empirical proof that brute-force dedispersion is a memory-bound algorithm, limited by low AI. In particular, we showed that achievable performance is limited by the amount of data reuse that dedispersion can exploit, and the available data reuse is affected by parameters like the DM space and the frequency interval. We also showed

that, even in a perfect scenario where data reuse is unrealistically high, the performance of dedispersion is limited by the constraints imposed by real hardware, and approaching the theoretical AI bound of the algorithm becomes impossible.

## References

- A. Hewish, S. J. Bell, J. D. H. Pilkington, P. F. Scott, R. A. Collins, Observation of a Rapidly Pulsating Radio Source, *Nature* 217 (1968) 709–713.
- D. R. Lorimer, M. Bailes, M. A. McLaughlin, D. J. Narkevic, F. Crawford, A Bright Millisecond Radio Burst of Extragalactic Origin, *Science* 318 (2007) 777.
- D. Lorimer, M. Kramer, *Handbook of pulsar astronomy*, 2005.
- T. H. Hankins, B. J. Rickett, *Pulsar Signal Processing*, in: *Methods in Computational Physics Volume 14 — Radio Astronomy*, Academic Press, New York, 55–129, 1975.
- J. van Leeuwen, B. W. Stappers, Finding pulsars with LOFAR, *A&A* 509 (26) (2010) 7, doi:10.1051/0004-6361/200913121.
- B. W. Stappers, J. W. T. Hessels, A. Alexov, K. Anderson, T. Coenen, T. Hassall, A. Karastergiou, V. I. Kondratiev, M. Kramer, J. van Leeuwen, J. D. Mol, A. Noutsos, J. W. Romein, P. Weltevrede, R. Fender, R. A. M. J. Wijers, L. Bähren, M. E. Bell, J. Broderick, E. J. Daw, V. S. Dhillon, J. Eislöffel, H. Falcke, J. Griessmeier, C. Law, S. Markoff, J. C. A. Miller-Jones, B. Scheers, H. Spreeuw, J. Swinbank, S. Ter Veen, M. W. Wise, O. Wucknitz, P. Zarka, J. Anderson, A. Asgekar, I. M. Avruch, R. Beck, P. Bannema, M. J. Bentum, P. Best, J. Bregman, M. Brentjens, R. H. van de Brink, P. C. Broekema, W. N. Brouw, M. Brügger, A. G. de Bruyn, H. R. Butcher, B. Ciardi, J. Conway, R.-J. Dettmar, A. van Duin, J. van Enst, M. Garrett, M. Gerbers, T. Grit, A. Gunst, M. P. van Haarlem, J. P. Hamaker, G. Heald, M. Hoeft, H. Holties, A. Horneffer, L. V. E. Koopmans, G. Kuper, M. Loose, P. Maat, D. McKay-Bukowski, J. P. McKean, G. Miley, R. Morganti, R. Nijboer, J. E. Noordam, M. Norden, H. Olofsson, M. Pandey-Pommier, A. Polatidis, W. Reich, H. Röttgering, A. Schoenmakers, J. Sluman, O. Smirnov, M. Steinmetz, C. G. M. Sterks, M. Tagger, Y. Tang, R. Vermeulen, N. Vermaas, C. Vogt, M. de Vos, S. J. Wijnholds, S. Yatawatta, A. Zensus, *Observing pulsars and fast transients with LOFAR*, *A&A* 530 (2011) A80+, doi:10.1051/0004-6361/201116681.
- C. L. Carilli, S. Rawlings, Motivation, key science projects, standards and assumptions, *New Astronomy Reviews* 48 (2004) 979–984, doi:10.1016/j.newar.2004.09.001.
- R. S. Foster, B. J. Cadwell, A. Wolszczan, S. B. Anderson, A High Galactic Latitude Pulsar Survey of the Arecibo Sky, *ApJ* 454 (1995) 826–830.
- M. J. Keith, A. Jameson, W. van Straten, M. Bailes, S. Johnston, M. Kramer, A. Possenti, S. D. Bates, N. D. R. Bhat, M. Burgay, S. Burke-Spolaor, N. D’Amico, L. Levin, P. L. McMahon, S. Miliã, B. W. Stappers, The High Time Resolution Universe Pulsar Survey - I. System configuration and initial discoveries, *mnras* 409 (2010) 619–627, doi:10.1111/j.1365-2966.2010.17325.x.
- T. Coenen, J. van Leeuwen, J. W. T. Hessels, B. W. Stappers, V. I. Kondratiev, A. Alexov, R. P. Breton, A. Bilous, S. Cooper, H. Falcke, R. A. Fallows, V. Gajjar, J.-M. Grießmeier, T. E. Hassall, A. Karastergiou, E. F. Keane, M. Kramer, M. Kuniyoshi, A. Noutsos, S. Osłowski, M. Pilia, M. Serylak, C. Schrijvers, C. Sobey, S. ter Veen, J. Verbiest, P. Weltevrede, S. Wijnholds, K. Zagkouris, A. S. van Amesfoort, J. Anderson, A. Asgekar, I. M. Avruch, M. E. Bell, M. J. Bentum, G. Bernardi, P. Best, A. Bonafede, F. Breitling, J. Broderick, M. Brügger, H. R. Butcher, B. Ciardi, A. Corstanje, A. Deller, S. Duscha, J. Eislöffel, R. Fender, C. Ferrari, W. Frieswijk, M. A. Garrett, F. de Gasperin, E. de Geus, A. W. Gunst, J. P. Hamaker, G. Heald, M. Hoeft, A. van der Horst, E. Juette, G. Kuper, C. Law, G. Mann, R. McFadden, D. McKay-Bukowski, J. P. McKean, H. Munk, E. Orru, H. Paas, M. Pandey-Pommier, A. G.

- Polatidis, W. Reich, A. Renting, H. Röttgering, A. Rowlinson, A. M. M. Scaife, D. Schwarz, J. Sluman, O. Smirnov, J. Swinbank, M. Tagger, Y. Tang, C. Tasse, S. Thoudam, C. Toribio, R. Vermeulen, C. Vocks, R. J. van Weeren, O. Wucknitz, P. Zarka, A. Zensus, The LOFAR pilot surveys for pulsars and fast radio transients, *aap* 570 A60, doi:10.1051/0004-6361/201424495.
- A. Magro, A Real-Time, GPU-Based, Non-Imaging Back-End for Radio Telescopes, Ph.D. thesis, University of Malta, Malta, 2014.
- E. Keane, B. Bhattacharyya, M. Kramer, B. Stappers, E. F. Keane, B. Bhattacharyya, M. Kramer, B. W. Stappers, S. D. Bates, M. Burgay, S. Chatterjee, D. J. Champion, R. P. Eatough, J. W. T. Hessels, G. Janssen, K. J. Lee, J. van Leeuwen, J. Margueron, M. Oertel, A. Possenti, S. Ransom, G. Theureau, P. Torne, A Cosmic Census of Radio Pulsars with the SKA, in: *Procs. AASKA14*, 9-13 June, 2014., 40, 2014.
- E. Petroff, M. Bailes, E. D. Barr, B. R. Barsdell, N. D. R. Bhat, F. Bian, S. Burke-Spolaor, M. Caleb, D. Champion, P. Chandra, G. Da Costa, C. Delvaux, C. Flynn, N. Gehrels, J. Greiner, A. Jameson, S. Johnston, M. M. Kasliwal, E. F. Keane, S. Keller, J. Kocz, M. Kramer, G. Leloudas, D. Male sani, J. S. Mulchaey, C. Ng, E. O. Ofek, D. A. Perley, A. Possenti, B. P. Schmidt, Y. Shen, B. Stappers, P. Tisserand, W. van Straten, C. Wolf, A real-time fast radio burst: polarization detection and multiwavelength follow-up, *mnras* 447 (2015) 246–255, doi:10.1093/mnras/stu2419.
- B. R. Barsdell, M. Bailes, D. G. Barnes, C. J. Fluke, Accelerating incoherent dedispersion, *Monthly Notices of the Royal Astronomical Society* ISSN 1365-2966.
- W. Armour, A. Karastergiou, M. Giles, C. Williams, A. Magro, K. Zagkouris, S. Roberts, S. Salvini, F. Dulwich, B. Mort, A GPU-based Survey for Millisecond Radio Transients Using ARTEMIS, in: *Astronomical Data Analysis Software and Systems XXI*, 2012.
- J. van Leeuwen, ARTS – the Apertif Radio Transient System, in: P. R. Woźniak, M. J. Graham, A. A. Mahabal, R. Seaman (Eds.), *The Third Hot-wiring the Transient Universe Workshop*, 79–79, 2014.
- S. Williams, A. Waterman, D. Patterson, Roofline: an insightful visual performance model for multicore architectures, *Commun. ACM* ISSN 0001-0782.
- A. Sclocco, H. E. Bal, J. Hessels, J. van Leeuwen, R. V. van Nieuwpoort, Auto-Tuning Dedispersion for Many-Core Accelerators, *Proceedings of the International Parallel and Distributed Processing Symposium (IPDPS)* ISSN 1530-2075.
- B. R. Barsdell, D. G. Barnes, C. J. Fluke, Analysing astronomy algorithms for graphics processing units and beyond, *Monthly Notices of the Royal Astronomical Society* .
- J. H. Taylor, A sensitive Method for Detecting Dispersed Radio Emission, *A&AS* 15 (1974) 367–369.
- R. N. Manchester, A. G. Lyne, F. Camilo, J. F. Bell, V. M. Kaspi, N. D’Amico, N. P. F. McKay, F. Crawford, I. H. Stairs, A. Possenti, D. J. Morris, D. C. Sheppard, The Parkes multi-beam pulsar survey - I. Observing and data analysis systems, discovery and timing of 100 pulsars, *MNRAS* 328 (2001) 17–35.
- K. Masui, H.-H. Lin, J. Sievers, C. J. Anderson, T.-C. Chang, X. Chen, A. Ganguly, M. Jarvis, C.-Y. Kuo, Y.-C. Li, et al., Dense magnetized plasma associated with a fast radio burst, *Nature* .
- Y. Li, J. Dongarra, S. Tomov, A Note on Auto-tuning GEMM for GPUs, in: *Computational Science ICCS 2009*, ISBN 978-3-642-01969-2, 2009.
- K. Datta, M. Murphy, V. Volkov, S. Williams, J. Carter, L. Oliker, D. Patterson, J. Shalf, K. Yelick, Stencil Computation Optimization and Auto-tuning on State-of-the-art Multicore Architectures, in: *Proceedings of the 2008 ACM/IEEE Conference on Supercomputing, SC ’08*, IEEE Press, Piscataway, NJ, USA, ISBN 978-1-4244-2835-9, 4:1–4:12, 2008.
- P. Du, R. Weber, P. Luszczek, S. Tomov, G. Peterson, J. Dongarra, From CUDA to OpenCL: Towards a performance-portable solution for multi-platform GPU programming, *Parallel Computing* ISSN 0167-8191, doi: http://dx.doi.org/10.1016/j.parco.2011.10.002.
- P. M. Phothilimthana, J. Ansel, J. Ragan-Kelley, S. Amarasinghe, Portable Performance on Heterogeneous Architectures, in: *Proceedings of the Eighteenth International Conference on Architectural Support for Programming Languages and Operating Systems, ASPLOS ’13*, ACM, New York, NY, USA, ISBN 978-1-4503-1870-9, 431–444, 2013.
- R. van Nieuwpoort, J. Romein, Correlating Radio Astronomy Signals with Many-Core Hardware, *International Journal of Parallel Programming* 39 (1) (2011) 88–114, ISSN 0885-7458.
- A. Sclocco, A. L. Varbanescu, J. D. Mol, R. V. van Nieuwpoort, Radio Astronomy Beam Forming on Many-Core Architectures, *Proceeding of the International Parallel and Distributed Processing Symposium (IPDPS)* ISSN 1530-2075, doi: http://doi.ieeecomputersociety.org/10.1109/IPDPS.2012.102.
- A. Magro, A. Karastergiou, S. Salvini, B. Mort, F. Dulwich, K. Zarb Adami, Real-time, fast radio transient searches with GPU de-dispersion, *Monthly Notices of the Royal Astronomical Society* ISSN 1365-2966.
- B. Zackay, E. O. Ofek, An accurate and efficient algorithm for detection of radio bursts with an unknown dispersion measure, for single dish telescopes and interferometers, *ArXiv e-prints* .